Title	Crystallographic Orientation of the Recrystallized Grain Grown in the Deformed Single Crystal of Ice
Author(s)	OHOTOMO, Mutsumi; 大伴, 武都美
Citation	Contributions from the Institute of Low Temperature Science, A34, 1-21
Issue Date	1985-03-30
Doc URL	https://hdl.handle.net/2115/20250
Type	departmental bulletin paper
File Information	A34_p1-21.pdf

Crystallographic Orientation of the Recrystallized Grain Grown in the Deformed Single Crystal of Ice*

by

Mutsumi OHOTOMO
大　伴　武都美
The Institute of Low Temperature Science

Received December 1984

Abstract

A single crystal of ice, shaped in a rectangle, with a grid of grooves on its top face was uniaxially compressed and then annealed to allow recrystallization. Although many recrystallized fine grains appeared at its grooved portion at the beginning of annealing, only a few grew into large grains invading the underneath portion in due time. It was found that the growth rate of a recrystallized grain depended linearly on the strain of the deformed matrix and also that a change occurred in activation energy at about 215 K, indicating a transformation in the structure of the grain boundary. The diffusion coefficient of recrystallization growth (namely, diffusion coefficient of the grain boundary diffusion) at 272.7 K, estimated from the growth rate, was in good agreement with the value deduced from a model of the melting grain boundary. Crystallographic orientation of the grown grains seemed to show some preferred orientation to the c-axis of the matrix, although the fine grains which appeared at the initial stage were randomly oriented. An attempt was made to interpret the origin of such a preferred orientation by proposing a growth model on the basis of the kinetic point of view.

Contents

I. Introduction

Flow in glaciers produces a wide variety of structures, small as well as large in scale, concerning the distribution and shape of air bubbles and the size, shape, and orientation of crystals. These features are referred to as ice fabrics in wide sense. As the flow of glaciers causes substantial role in them, from it arises the possibility of interpreting the deformational history of a piece of glacier ice by studying its texture and fabrics. From such a point of view, many samples from various glaciers have been studied by many researchers. If we limit ourselves to the studies on the preferred orientation of crystallographic axes (namely, fabrics in a narrow sense), Bader (1938), and Perutz and Seligman (1939) started measuring of the crystallographic orientation of glacier ice. Many investigations for the samples from various locations, for example, Rigsby (1951, 1955, and 1960), Kamb (1959), and Kizaki (1962, 1969a and b) followed; through their observations they proposed the hypothesis that the development of the preferred orientation, the main cause of which is the recrystallization process, is controlled fundamentally by the type of stress, total strain, and temperature.

To help clarify the matter in point, the structural changes produced by various stress systems have been studied in the laboratory as follows: Kamb (1972), pursuing earlier studies by Steinemann (1958), Shumskii (1958), and Rigsby (1960), deformed polycrystalline ice to allow the recrystallization at stresses of a few hundred KPs at temperatures between 0 and $-5°C$. The crystals were randomly oriented at the start of the experiment. Recrystallization began at a strain of a few per cent. In simple shear the recrystallized c-axis fabrics had two maxima. Recently, Wilson and Russel-Head (1982) investigated the steady state profile of the preferred orientation of the recrystallized c-axis in the stress field. Despite the foregoing investigations, however, the knowledge of it is far from complete. For example, the formation mechanism of the fabrics of ice near the base of temperate and some polar glaciers consists of three of four maxima, called the triangle or diamond pattern, is not well explained.

Experimental study made thus far have two characteristics in common: the use of polycrystalline samples and the aim to show the result of the recrystallization process but not the process of it. In the case of the polycrystal, however, the interaction between grains of the sample have prevented from clarifying the fundamental mechanism of the recrystallization. Thus, we carried out experiments, which causes recrystallization to occur in a single crystal of ice. Furthermore, we aimed at observing the process of growth, after the earlier studies by Wakahama (1964 and 1965).

For obtaining the total picture of the formation mechanism of the preferred orientation in polycrystal by recrystallization, the growth rate is as fundamental as the crystallographic orientation. The present paper describes first the experiment to examine the dependence of the growth rate of a recrystallized grain on temperature and driving force. In this

connection, the value of the diffusion coefficient of the growth (namely, grain boundary diffusion coefficient) estimated from the obtained growth rate was found considerably larger than that of the volume diffusion coefficient in ice, and was found rather comparable to that of water. Besides, a change in activation energy for recrystallization growth was found. So a nucleation magnetic resonance (NMR) test was conducted to check the structure of the growth interface of recrystallization (namely, grain boundary). On the basis of these results, a model of the grain boundary in ice near the melting point is proposed; then the thickness and free energy of it are discussed.

Next, the experiment aimed at clarifying the crystallographic orientation of a recrystallized grain is described. The result of the experiment shows that many fine recrystallized grains which appeared at the initial stage scarecely had the preferred orientation; however, the c-axis of the grown grain was related to that of the matrix, contrary to the results reported by others to date. In case of metals this result seems to be explained by the C. S. L. (Coincidence Site Lattice) theory (Kronberg and Wilson 1949). However, in case of this experiment, the result was not explained by the theory. Hence, in an effort to explain the result a kinetic theory of recrystallization is proposed, with some success. Finally, an attempt is made to interpret the misorientation relation between adjoining grains of the multiple maxima fabrics pattern (namely, triangle or diamond pattern) using the experimental result.

II. Experimental Procedure

II. 1. *Sample and growth method*

A rectangular solid sample was cut from a large-sized single crystal of ice from Mendenhall Glacier (Higashi et al., unpublished), which contained so little impurities as given in Table 1 (Higashi, 1971). The sample was used for all the experiments under various conditions. A

Table 1 Impurities of ions contained in the single crystal of ice after Higashi (1971).

			ppm
Cl	Ca	Mg	SO$_4$
0.2	1.5	0.02	0.8

sample cut from it was uniaxially compressed and subjected to annealing. Then a recrystallized grain was grown in the sample, although the actual procedures for its growth differ slightly from one another as are described later.

II. 2. *Growth rate of the recrystallized grain*

Driving force dependence of recrystallization growth A sample about $4 \times 5 \times 5$ cm^3 was cut out in such a manner that its c-axis was parallel to its top face. Then, the sample was compressed uniaxially normal to the stress axis. A pick with a pin on the surface of a sliced test piece usually caused nucleation in it. It was annealed for 3 hours at 272.7 K in an annealing box set under a polarizing microscope. The growth process of the nuclei during

the annealing was recorded with a series of time-lapse photographs. Data obtained from the first 30 minutes were omitted so that the effects of the stress-concentrated area as a result of the picking was avoided. In addition to this, as the growth rate decreases with a lapse of time due to the recovery process of the test piece, the obtained value of growth rate is the mean value for 2.5 hours. As the recrystallized grain showed anisotropy in growth rate, the growth rate of the fastest migrating grain boundary was measured for each grain.

The dislocation density of the deformed matrix was determined by the etch pit density method (Kuroiwa and Hamilton, 1962) after annealing.

Temperature dependence of recrystallization growth rate A somewhat different procedure from the previous section was adopted for this experiment as follows: The c-axis of a sample was chosen for the top face, as described in the previous section. Next, using a band saw, we cut grooves in a gridiron pattern on the top face. Then, the sample was compressed uniaxially normal to the top face by about 20% at 263 K. During the deformation the grooves on the top face were closed due to stress concentration in the portion. After deformation, the sample was sliced to a thickness of 3 mm parallel to the stress axis and sliced test pieces were annealed in an annealing box at a constant temperature. Some of a large number of recrystallized nuclei, formed at the grooved portion where the stress was concentrated, started growing toward the deformed matrix. The test pieces were annealed in the temperature ranging from 83 to 272.7 K. The annealing period was 24 hours above 253 K; however, below 253 K it was 100-200 hours, because otherwise the growth would not be detected. After annealing, a photograph was taken under the polarizing microscope to record the displacement of the grain boundary. Growth rate of the fastest migrating grain boundary of each recrystallized grain was also obtained from photographs taken before and after the annealing. The obtained data for the growth rate represent the mean value of the annealing period like in the case of the experiment of the driving force dependence.

II. 3. *An NMR test for recrystallized grains*

As mentioned later, it is considered that a transformation in the structure of the grain boundary in ice near the melting point results from the melting of the grain boundary. Hence, an NMR test was made to check the transformation using a wide-line NMR spectrometer. Test pieces were prepared by the following procedures: A rectangular solid sample of a single crystal of ice, about $4 \times 4 \times 10$ cm³, was cut out from a single crystal; then it was deformed uniaxially by 90 % at 263 K; a test piece was prepared from it. After that, we immediately mounted the test piece on the apparatus. As a large number of recrystallized grains appeared during the deformation, the test piece had a large sum of specific area of the grain boundary in it. Moreover, it had many growing recrystallized grains.

II. 4. *Crystallographic orientation of the recrystallized grain*

Crystallographic orientation of the recrystallized grain The growth procedure adopted

Table 2 Experimental conditions

Size of Sample mm	Total strain %	Strain rate $\times 10^{-6} s^{-1}$	Yield stress KPa	Number of obtained new grains
38x53x80	17.9	0.04	387	2
51x39x79	22.0	0.05	739	2
46x42x88	27.5	0.947	608	4
61x42x82	28.0	1.01	425	1
50x41x40	10.0	2.08	1431	7
38x52x45	15.6	1.86	2726	9
61x39x79	22.0	1.05	739	2
56x42x88	27.5	0.947	608	1
34x37x26	24.2	3.20	386	1
49x43x20	20.0	4.17	744	6
66x37x33	15.1	2.51	241	2
47x26x43	12.3	1.93	201	1
42x50x39	15.4	2.14	838	8
66x37x33	15.1	2.51	602	2
48x37x32	14.0	2.59	386	1
50k58x28	15.0	2.98	607	2
40x49x32	11.0	2.60	250	2
45x54x25	18.8	3.33	483	4
40x49x32	11.0	2.60	250	2
40x47x24	20.8	3.47	487	2

here is almost the same as that described in the experiment of measuring the temperature dependence of the growth rate. It should be noted, however, that the c-axis of the matrix, which was determined by the transmission Laue method, was chosen relative to the compression axis. Furthermore, the sample was annealed without slicing. Irrespective of the straining conditions shown in Table 2, by the annealing at 272.7 K ($T/T_m = 0.999$, T_m: melting point), spontaneous nucleation occurred only in the grooved portion (the nucleation region), where many nuclei appeared, of which a few could grow into large grains invading the less-strained matrix (the growth region). The crystallographic orientations of the grown grain and also of the deformed matrix were determined by the transmission Laue method after annealing. No appreciable change was found in the orientation of the matrix by the compression.

Origin of the orientation relation A few additional experiments were conducted to study the orientation distribution of fine recrystallized grains which appeared in the grooved portion and also to observe the growth interface. For the first purpose, the fine recrystallized portion was cut out from the compressed sample and its Debye-Scherrer photograph was taken. For the second, a section more than 5 mm in thichness was cut out from the compressed sample parallel to the compression axis, and then annealed at 272.7 K in an

annealing box. By using a thick section like this, the recrystallized grain was capable of growing without an effect from the surface. Subsequently the grain boundary orientation was determined using a universal stage; then crystallographic orientations of two interfaces of grains which were bounded by such a grain boundary were determined.

III. Result of Experiments

III. 1. *Growth of the recrystallized grain*

A recrystallized grain grown in the deformed single crystal of ice, whose thin section was cut normal to the compression axis, is given in Fig. 1. Photographs taken in the successive growth stages of recrystallization of a strained specimen under a polarizing microscope are shown in Fig. 2. Figure 2-a, taken two hours after the beginning of annealing, already showed many fine grains. Most of them simply disappeared in the later photographs, and only a few grew further, invading the matrix. At the subsequent stage of the growth, the grain continued to have a curved grain boundary (Fig. 2-b). At the later stage (Fig. 2-c), the grain developed facets showing some anisotropy in growth rate.
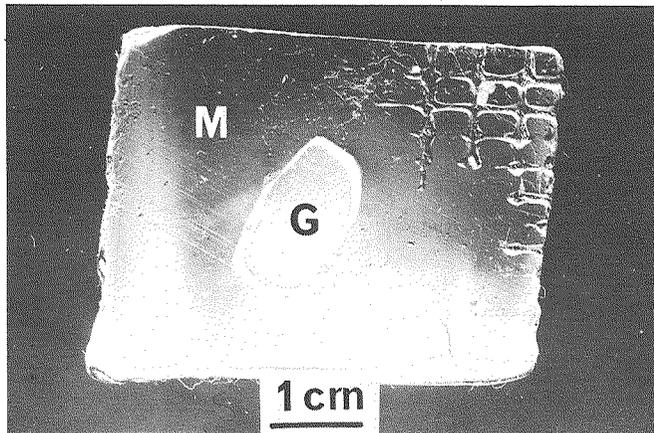

Fig. 1　Polarizing photograph of a recrystallized grain grown in the deformed single crystal of ice, whose thin section was cut normal to the compression axis. M: The deformed matrix; G: the recrystallized grain. Annealing temperature was 272.7K.

III. 2. *Growth rate of the recrystallized grain*

Driving force dependence of recrystallization growth Figure 3 shows the dependence of the recrystallization growth rate on the driving force when the sample was deformed within 2-20%. It becomes evident that the growth rate changes linearly with the strain on the
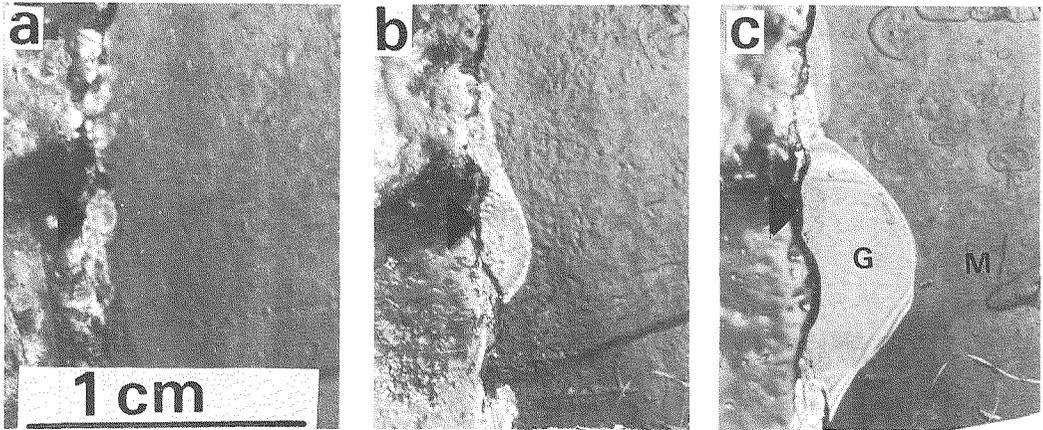
Fig. 2   Different stage of recrystallization under crossed polaroids.   M: the deformed matrix;
G: the recrystallized grain.   a: after 2 hours; b: after 60 hours; c: after 72 hours.
Annealing temperature was 272.7K.

matrix, as indicated in the figure.

The dislocation density of the deformed matrix was within the order of $10^6 - 10^7$ cm^{-2} after annealing in the case of deformation by 5%. The growth rate of the recrystallized grain at the strain was within $0.035 - 0.065$ mm/h. Measurements were made of the dislocation density in almost all the samples. For samples deformed by a strain of more than 8%, however, the sensitivities of the microscope and the method used made it difficult to make accurate measurements of the dislocation density.   The reason why the measured values of dislocation density were not accepted in case of the deformation by 2% is that the measured value of growth rate deviated from the line as shown in Fig. 3.

Fig. 3   Driving force dependence on growth rate of the recrystallized grain at 272.7K.

Temperature dependence of recrystallization growth rate   The recrystallization growth rate and its temperature dependence are indicated in Fig. 4.   It is revealed that this dependence shows a chang near 215 K.   The activation energy obtained for the growth rate of the recrystallized grain was 0.5 eV at temperatures not lower than 215 K and 0.02 eV between 215 K and 83 K.
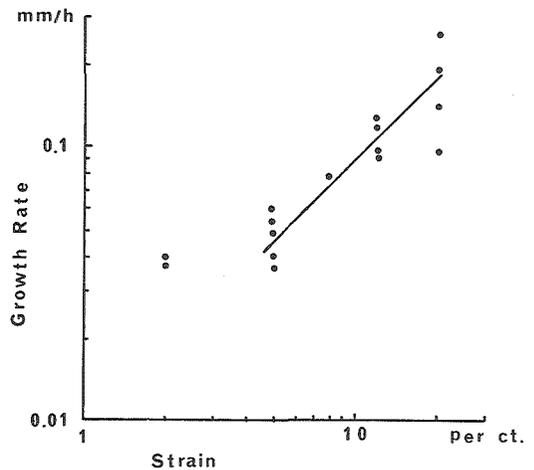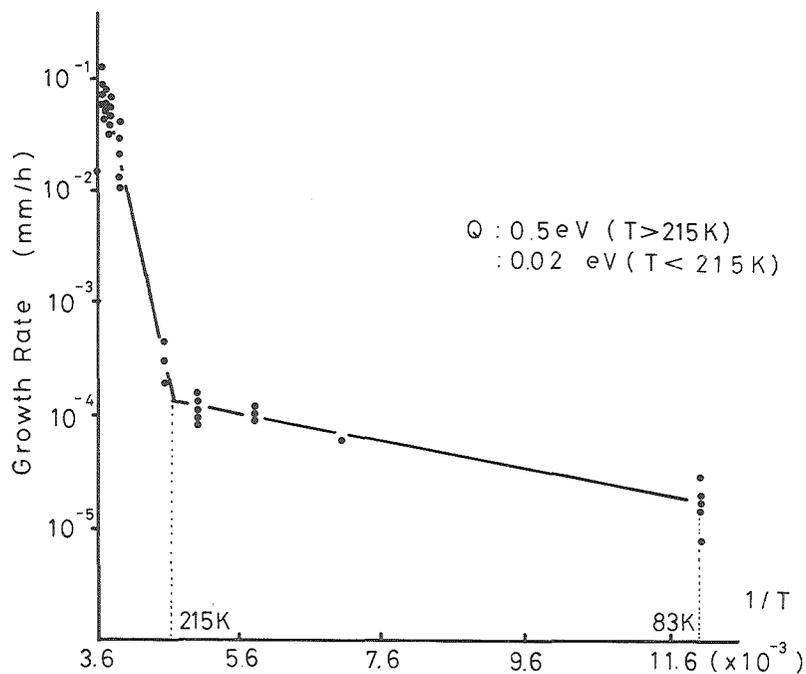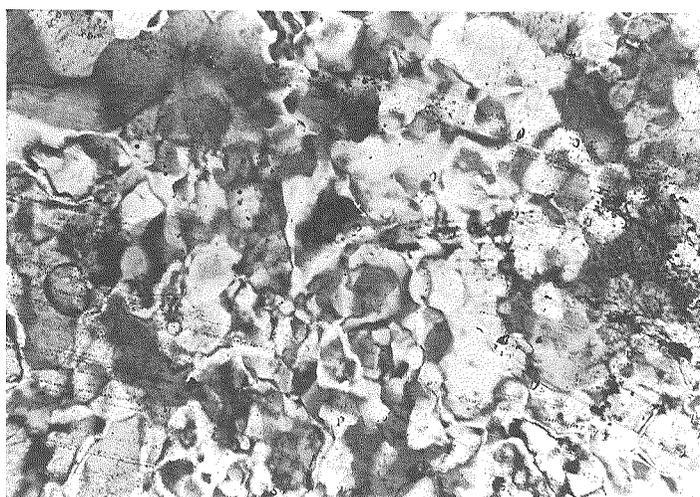
Fig. 4   Log recrystallization growth rate vs. $1/T$ (K).

5 m m

Fig. 5   Photograph of a thin section of an NMR test piece taken under crossed polarizers.
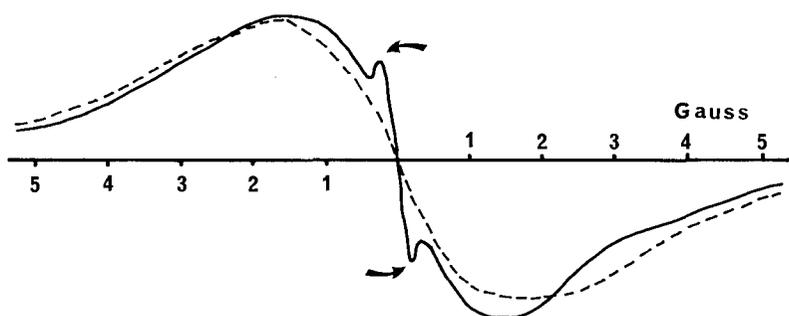
Fig. 6   Signals from an NMR test piece. Solid line at 272.7K; broken line at 270K. The peak is indicated by the arrow.

III. 3. *An NMR test for recrystallized grains*

Figure 5 shows a photograph of a thin section of a polycrystalline test piece for an NMR study taken under crossed polarizers.   The mean diameter of the grain is 0.2 mm, and the specific area of the grain boundary is estimated to be within 0.01—0.1 m²/g.   The result of the NMR tests are indicated in Fig. 6.   In this figure the solid and the broken line give the result at 272.7 K and 270 K, respectively.   No experiment was conducted above 272.7 K to prevent the test piece from fusing.   It is evident from Fig. 6 that only at 272.7 k the test piece shows a narrow component denoted by an arrow.   The relative intensity of the narrow component in the NMR spectra is 0.3%.   No peak appeared below 270 K, however.

III. 4. *Crystallographic orientation of the recrystallized grain*

In total 20 samples were tested, whose c-axis relative to the compression axis, are given in Fig. 7 by a stereographic projection, where the solid circles represent their c-axis and four solid triangles indicate the orientations of the corners of their top face.

The crystallographic orientations of the 61 recrystallized grains grown in the deformed matrices are given relative to the compression axis by a stereographic projection in Fig. 8, and relative to those of their matrices by a stereographic projection in a 1/6 fan shape in Fig. 9.   In Fig. 8, the solid circles show the c-axis, the open circles the a-axes, and the center of the projection circle
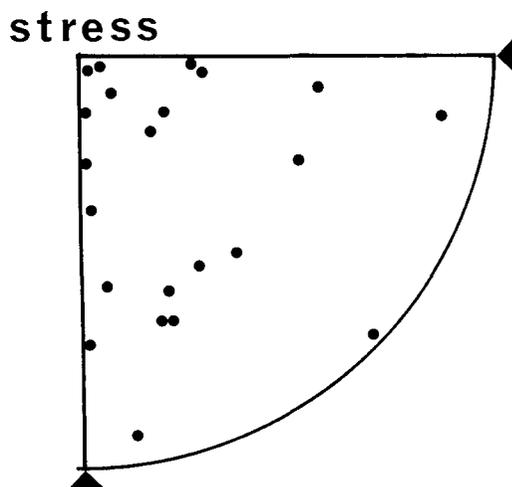

stress

Fig. 7   Chystallographic orientation of the c-axis of a sample in a quadrant of the standard projection. Center of the projection circle is related to the compression axis.
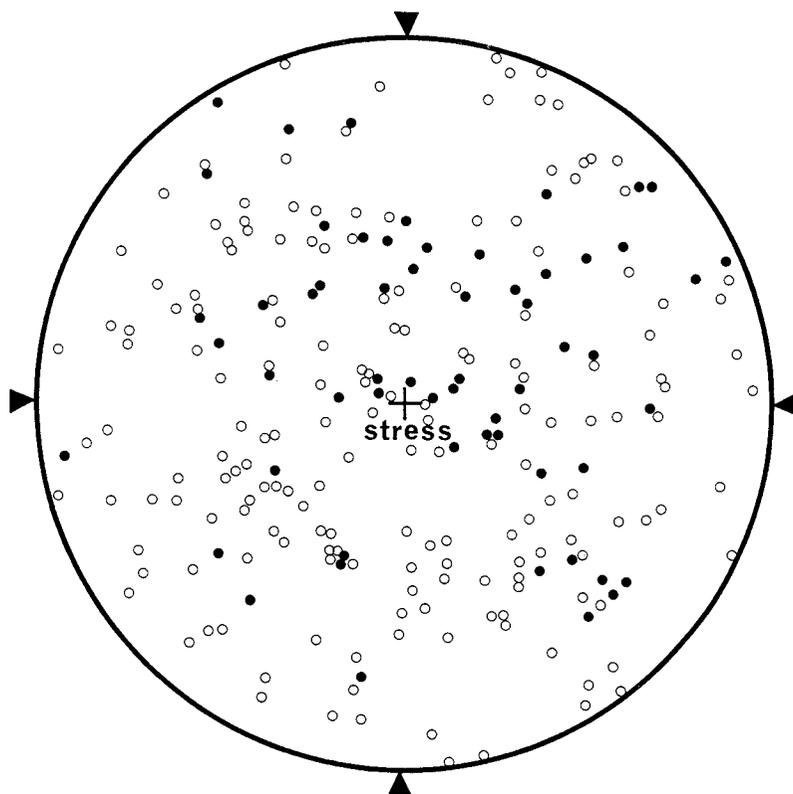
Fig. 8 Orientation relation of the artificially nucleated grains to the compression axis
as the center of the circle in the standard projection.
● : Orientation of a c-axis of the recrystallized grain.
○ : Orientation of a a-axis of the recrystallized grain.
▲ : Orientation of the corner of the top face of the sample.

the compression axis. Meanwhile, Fig. 9 is constructed as follows: Of nine pairs of the
a-axes of the matrix and the a-axes of the recrystallized grain, the pair making the smallest
misorientation was chosen. The a-axes of the matrix of the pair is placed at the point
denoted by $[11\bar{2}0]_M$ or $[2\bar{1}\bar{1}0]_M$ while the c-axis of the matrix is denoted by $\langle 0001 \rangle_M$ at the
center in Fig. 9. Then, the c-axes of the recrystallized grains are plotted on the figure by
solid circles and the a-axes of the grains of the pair by open circles related to the a-axis of
the matrix of the pair.

Contrary to the expectation from the results of studies by other reseachers, the c-axes
of the grains do not depend upon the compression axis, as shown in Fig. 8. The misorien-
tations of the c-axis between the grains and their matrices, given in Fig. 9, have a peak
around 50°, though the fine grains were randomly distributed as seen from the Debye-Scherrer
photograph of the nucleation region immediately after the compression as indicated in
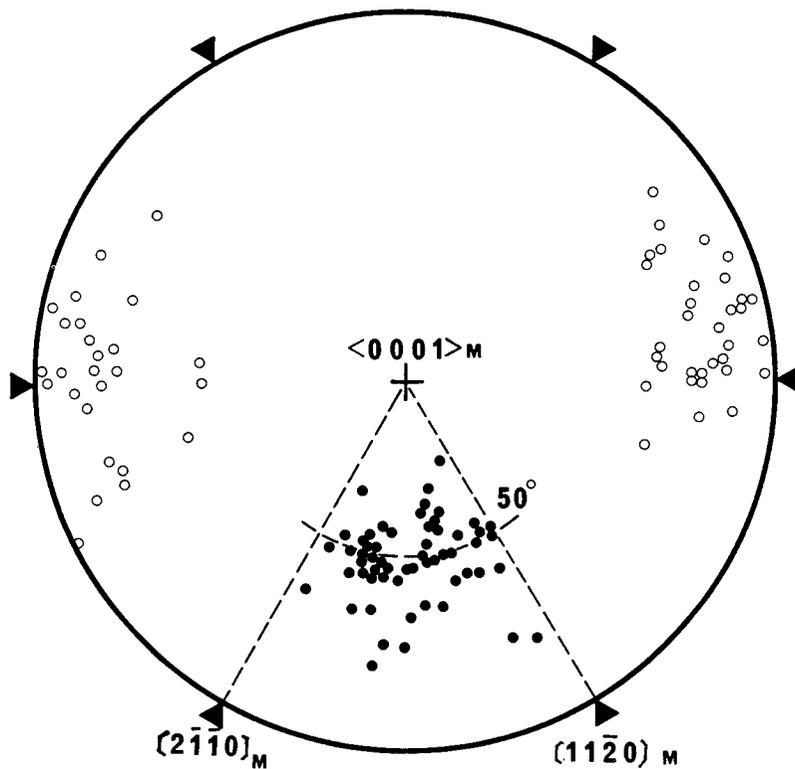
Fig. 9   Orientation relation between the recrystallized grain and the deformed matrix
          in a 1/6 fan shape of the standard projection.   The center of the circle is the
          c-axis of the deformed matrix.   The broken line shows a misorientation of 50°
          from the center.
          ● : Orientation of the c-axis of the recrystallized grain.
          ○ : Orientation of a a-axes of the recrystallized grain, which has the smallest
              misorientation related to the a-axes of the deformed matrix.

Figure 10.

As seen from Fig. 9, neither c-axis nor a-axis of the recrystallized grain coincided with
the corresponding axis of the matrix.   A further examination showed that the matrix and
the recrystallized grain shared neither other low-indexed axis nor low-indexed plane.

Crystallographic orientations of facets developed during the growth, whose photographs
are shown in Fig. 2, are given in Fig. 11 by the similar style to Fig. 9.   Figures 11-a and -b
give the crystallographic orientations of the fastest and the slowest segment of the migrating
grain boundary in a growing grain looked out of the matrix side and the grain side, re-
spectively.   Though only three data of measurements were obtained for both segments, it
appears that the orientation of the fast migrating grain boundary segment at the later stage
is related to the plane near the pyramidal plane of the matrix and the plane nearly parallel

to the c-axis of the grain, and in the case of the slow migrating grain boundary segment, one of them is related to the plane near the basal plane.
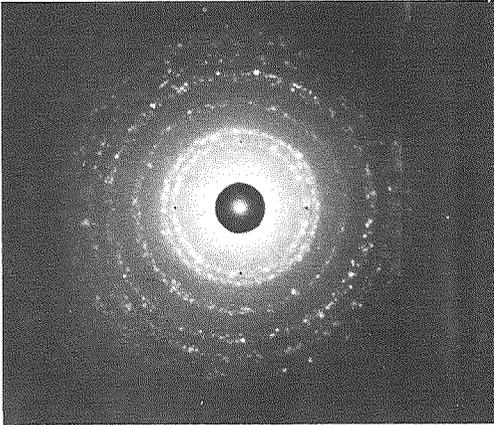

Fig. 10   Debye-Scherrer photograph of fine recry-
stallized grains of the cut portion of the
matrix before annealing. Large spots
originate from grains with a relatively
large grain size.
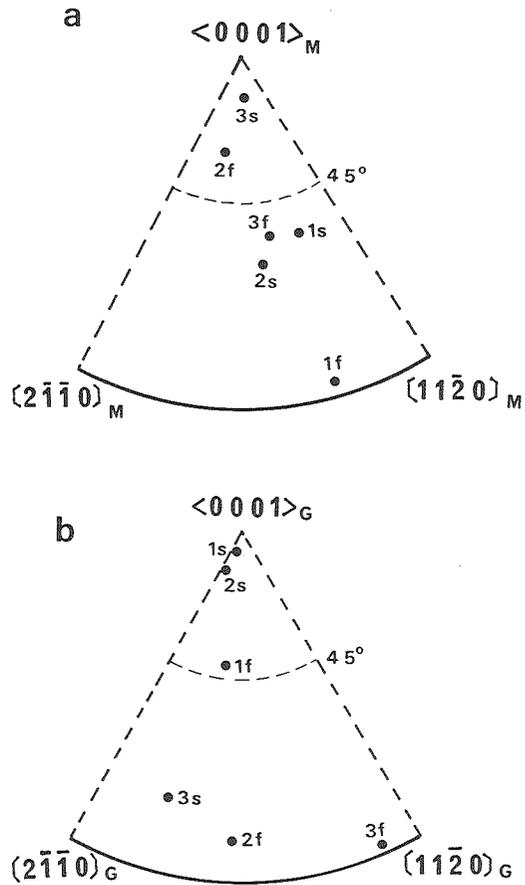
Fig. 11   Crystallographic orientation of the grain
boundary in the standard projection using
a 1/6 fan shape. "f" and "s" denote the
fastest and the slowest migrating grain
boundary, respectively.
a : Pole of the grain boundary looked out
of the deformed matrix. The center is
related to the c-axis of the matrix.
b : Pole of the grain boundary looked out
of the recrystallized grain. The center is
the c-axis of the recrystallized grain.

IV. **Discussions**

IV. 1. *Growth rate of the recrystallized grain*

As shown in Fig. 3, the growth rate of recrystallization in ice at 272.7 K depends linearly upon the total strain of the deformed matrix.   This dependence implies that the growth rate is characterized not by growth kinetics, but by diffusion of water molecules which contributes to the growth.

The dislocation density of the deformed matrix obtained by the etch pit density method is of the order of $10^6 - 10^7$ cm², which gives a driving free energy of recrystallization (e. g., Gleiter and Chalmers 1972) in a range from 6×10 to 6×10^2 erg · cm⁻³ or from 2×10^{-21} to 2×10^{-20} erg/atom.   For the growth rate of 0.05 mm/h and the free energy in this range, the diffusion coefficient for recrystallization growth (namely, grain boundary diffusion coefficient), D_R, at 272.7 K was calculated after Turnbull (1951) as $1 \times 10^{-6} - 1 \times 10^{-7}$ cm²/s, where the jumping distance of a water molecule is assumed to be 4.5×10^{-8} cm.   It should be noted that this value of D_R differs greatly from the value of the volume diffusion coefficient of ice (e. g., Fletcher 1970), and is rather close to that of water, which is of the order of 10^{-5} cm²/s (Eisenberg and Kauzmann, 1969).   It implies that the recrystallized grain grew as if from the melt phase.   The growth interface of recrystallization (grain boundary) must have a large number of mobile water molecules as assumed in the theory of grain boundary melting (e. g., Gleiter and Chalmers op. cit.).

The change in value of activation energy for the growth of recrystallization near 215 K ($T/T_m = 0.79$; T_m: melting point), as shown in Fig. 4, suggests that the structure of the grain boundary underwent a transformation below near $0.8 T_m$, as indicated in some materials (Aust, 1969; Demianczuk and Aust, 1975).

IV. 2. *The Mobile water phase in the grain boundary*

The existence of a quasi-liquid layer at the surface of ice has been revealed experimentally by an NMR and other methods (Kvlividze et al., 1974; Beaglehole and Nason, 1980). Kvlividze et al. already showed the existence of the mobile water phase in the polycrystalline ice; however, they concluded that it does not exist in the grain boundary, but only at the surface.   The peak, which is considered to have originated from the mobile water phase, was also detected in the present experiment.   Because the sample used here contained few bubbles (namely, surfaces), it is considered possible that the mobile water phase has existed in the grain boundary (grain boundary melting).   This possibility further supports the discussion in the previous section.   As the reason why the peak did not appear at 270 K it is supposed that the total specific area of mobile water molecules was too small to be detected because the test piece had a much smaller specific area of the grain boundary than that of Kvlividze.   It is an unsolved problem to find a temperature, at which the mobile water phase

can exist, as well as the nature of it.

IV. 3. *A model of the grain boundary in ice near the melting point*

A model of the grain boundary of ice near the melting point is now proposed according to the discussions in sections IV. 1 and 2. The model is characterized by the wide grain boundary (Bolling, 1968; Lücke et al. 1972), which has mobile water molecules and will be mentioned again in section IV. 5.

IV. 4. *Thickness and free energy of the grain boundary in equilibrium*

The existence of the melt phase below the melting point brings about a disadvantage in stability because of the bulk free energy of a system. The factor which contributes to making the water phase thermodynamically stable despite this disadvantage can be explained by a decrease in the free energy of the interface due to the existence of such a phase in the grain boundary of an ice crystal. Kuroda and Lacmann's discussions (1982) on a quasi-liquid layer existing on the ice surface are expanded to treat the water phase which exists in the grain boundary as follows: The wettability parameter, $\Delta\gamma_\infty$, is defined in this case by the following expression:

$$\Delta\gamma_\infty = \gamma_{cc} - \{\gamma_{lc}^{(1)} + \gamma_{lc}^{(2)}\} \tag{1}$$

where γ_{cc}, $\gamma_{lc}^{(1)}$, and $\gamma_{lc}^{(2)}$ are respectively the amount of free energy of the grain boundary between ice (1) and ice (2), that between ice (1) and water, and that between ice (2) and water. If $\Delta\gamma_\infty > 0$, a melt layer is capable of existing in a stable state in the grain boundary. The total free energy $\Delta f(\delta)$ of the grain boundary is given by the following as a function of the thickness δ of the water layer:

$$f(\delta) = \gamma_{lc}^{(1)} + \gamma_{lc}^{(2)} + \frac{A^n}{(A\delta)^n}\Delta\gamma_\infty + \frac{\delta}{V_m}\frac{Q_m}{T_m}\Delta T \tag{2}$$

where T_m is the melting point of ice; Q_m is the molecular heat of melting of ice; V_m is the molecular volume of water in the grain boundary layer; $\Delta T = T_m - T$ represents the degree of supercooling; A and n are parameters which should be determined by microscopic studies or further experiments.

Equilibrium is attained between the ice and the water layer when Δf is at its minimum ($\delta = \delta_{st}$). The equilibrium thickness δ_{st} is given by

$$\delta_{st} = -A + \left[\frac{nA^n\Delta\gamma_\infty V_m T_m}{Q_m\Delta T}\right]^{1/(n+1)} \tag{3}$$

The chemical potential, μ_{gb}, of the grain boundary referred to that of ice is given by partially differentiating $\Delta f(\delta)$ by the number of molecules as follows:

$$\Delta \mu_{gb}(\delta) = \Delta T \left[\frac{Q_m}{T_m} \right] - \frac{n A^n \Delta r_\infty V_m}{(A+\delta)^{n+1}} \tag{4}$$

Then, we can estimate the thickness and free energy of the grain boundary in ice near the melting point as follows: The value of γ_{lc} between ice and water can be obtained on an assumption that the interfacial free energy, γ_{lc}, is proportional to the surface energy, γ_c, and the proportion, γ_{lc}/γ_c, is equal to the ratio of heat of fusion to heat of sublimation. The results of the calculation by Akutsu and Ookawa (unpublished) of anisotropy in the surface energy of ice using the broken bond method are utilized for estimating the thickness and free energy of the grain boundary which is constructed by two $\{11\bar{2}3\}$ planes as follows: As γ_c $\{11\bar{2}3\}$ $= 191.0$ erg/cm² and $\gamma_{cc} = 2\gamma_c = 382$ erg/cm², then γ_{lc} $\{11\bar{2}3\} = 22.4$ erg/cm². The grain boundary free energy at 272 K is 60 erg/cm² from eq. (2), which is close to the experimental value, 65 ± 3 erg/cm² (Ketcham and Hobbs, 1969), at the melting point, where $A = 1.5 \times 10^{-8}$ cm; $n = 1$; $V_m = 3.0 \times 10^{-23}$ cm³; $Q_m = 1 \times 10^{-13}$ erg/atom; and $T_m = 273.15$ K. From eq. (3), the resultant value of the equilibrium thickness of the grain boundary, δ_{st}, is 6.3×10^{-7} cm at 272 K. It decreases with falling temperature to the thickness of 7.0×10^{-8} cm at 215 K ($0.79 \cdot T_m$), that is almost of the order of the lattice space of the ice crystal. Although the experimental knowledge of the grain boundary of ice is by no means satisfactory now, at least values of thickness, free energy, and anisotropy in them are obtainable by the present method.

IV. 5. *Orientation relation between the recrystallized grain and the matrix*

A growth model of recrystallization As the fine recrystallized grains are distributed randomly at the initial stage of its growth, the crystallographic orientation of the grown grains should be characterized at the subsequent stage of growth, as suggested by Beck (1954). It becomes evident in this experiment that the c-axis of the recrystallized grain cannot be related to the stress axis, contrary to the results from obtained by other reseachers. The discrepancy between the result of the present study and those of the others is considered as follows: The orientation of the c-axis of the recrystallized grain depends upon that of its matrix which represents each grain in case of a polycrystal; however, the growth rate of the recrystallized grain also plays the substantial role in determining the distribution of c-axes in the polycrystal. As the strain energy stored in the matrix controls the growth rate, the rate would be affected by anisotropy in deformation of the matrix. For example, if a matrix (namely, a grain in the polycrystal) has less strain energy than other matrices, it is likely that a recrystallized grain which appears in the matrix does not grow predominantly. The preferred orientation of the c-axes of the polycrystal which appears as a result of the recrystallization is considered to be a superposition of these individual growth processes.

Differing from the result in metals (Yoshida et al., 1959; Ibe and Kücke, 1960; Watanabe, 1983), the recrystallized grain and the matrix did not have any low-indexed crystallographic
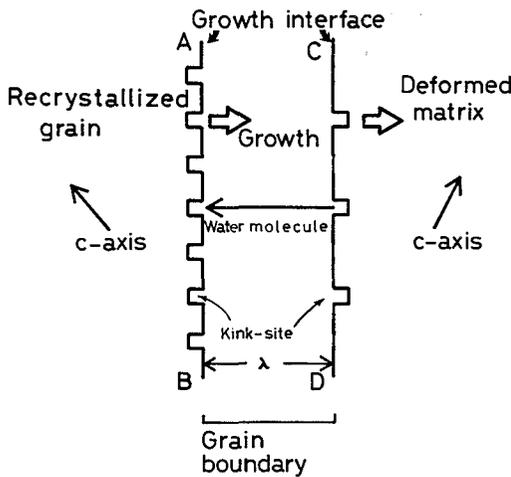
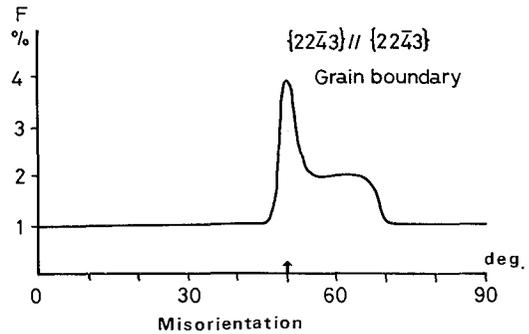Fig. 12   A model of recrystallization growth in ice.

Fig. 13   Misorientation angle between c-axes of two adjoining crystals vs. frequency in per cent. Two crystals are joined by two planes of the form { $22\bar{4}3$ }, and rotated around the pole of the grain boundary at the interval of 0.1°. An arrow denotes the case of a pure tilt.

axis or plane in common; and hence the preferred orientation of the grown grains relative to the matrix cannot be explained by the C. S. L. on the basis of the condition of equilibrium. Therefore, an attempt is made to explain it from the kinetic point of view.   We suppose the grain boundary of the recrystallized grain has two growth interfaces filled with mobile water molecules as described in the previous section and shown schematically in Fig. 12.   Both interfaces (A-B and C-D in Fig. 12) have kink-sites on them.   A water molecule is removed from kink-site of interface C-D due to the strain energy of the deformed matrix, and then attached to the kink-site of interface A-B.   Growth of the recrystallized grain is due to the migration of both interfaces in the rightward direction in the figure; then the growth rate is controlled by one of the interfaces which has a smaller kink-density in the steady state.

The kink density on the interface (namely, surface in this discussion) of ice is estimated geometrically, considering an intersection plane cutting the structure of an ice crystal. Then, the number of broken bond sites per unit area and the number of its first nearest broken bond sites per unit area were calculated, the results of which are listed in Table 3. An oxygen atom of ice has four first nearest bonds; therefore, a kink-site has two survived bonds.   The kink density tabulated here is expressed by the ratio of the number of kink-sites to that of broken bond sites (including kink-sites).   It becomes evident that the planes of a zone which are parallel to the zone axis $\langle 10\bar{1}0 \rangle$ have the largest kink-density and furthermore, that the $\{11\bar{2}2\}$ plane has the highest kink-density in all of the crystallographic planes in ice. A further examination reveals that the kink-density of a high-indexed plane, which is not tabulated, differs slightly from that of a low-indexed plane close to it.

Application of a growth model to the interpreatation of the orientation relation   As many

Table 3   Kink-density on the surface of an ice crystal.

Index of plane	Number of kink-sites per unit plane	Misorientation angle from the ⟨0001⟩ axis (deg.)	Kink density per unit area
{11$\bar{2}$0}	0	90.0	0
{22$\bar{4}$1}	2	81.2	1/8
{112$\bar{1}$}	2	72.9	1/4
{22$\bar{4}$3}	6	65.2	1/3
{11$\bar{2}$2}	2	58.4	1/2
{11$\bar{2}$3}	4	47.3	1/3
{11$\bar{2}$4}	2	39.1	1/3
{10$\bar{1}$0}	0	90.0	0
{20$\bar{2}$1}	2	75.1	1/4
{10$\bar{1}$1}	2	61.9	1/3
{10$\bar{1}$2}	1	43.1	1/3
{10$\bar{1}$3}	2	32.0	1/5

fine recrystallized grains which appeared at the initial stage have random orientations, they may have exery combination of interface A-B and interface C-D both interfaces having crystallographic orientations of all the indeces.   A fine recrystallized grain, which has a segment of the grain boundary adjoined by highly kinked interfaces, is capable of growing invading the deformed matrix.   It follows that the obtained orientation relation between the grown recrystallized grain and the deformed matrix is characterized by such a fine grain. For example, when a fine recrystallized grain has a segment of the tilt grain boundary adjoined by two {11$\bar{2}$2} planes, which have the largest kink density, the grain has the largest possibility of growing.   If so, the resultant misorientation angle between the c-axes, which is calculated from the misorientation between the c-axis and the pole of the plane given in Table 3, namely in case of {11$\bar{2}$2}// {11$\bar{2}$2} is 62°; in case of a tilt grain boundary of {22$\bar{4}$3}// {22$\bar{4}$3} it is 50°; in case of another tilt grain boundary of {10$\bar{1}$1}// {10$\bar{1}$1} it is 56°.   The experimental result given in Fig. 9 shows that these angles appesrs in high frequencies.

   In addition to this discussion, we also need to consider a twist component of the grain boundary in a general discussion of the relative misorientation between two grains as follows: When two grains bounded by a certain grain boundary are twisted around the pole of the grain boundary, misorientation angles between the two grains will change.   We simulated the change between the c-axes of both.   One of the results is shown in Fig. 13: A plane of the planes of the form {22$\bar{4}$3} was adjoined to another, then twisted around the pole of the plane (namely, grain boundary).   We calculated the misorientation angle during the twisting at intervals of 0.1° for every combination of the planes of the form {22$\bar{4}$3} .   Finally, the calculated results were summed up.   As shown in Fig. 13, the misorientation angle indicating its maximum frequency almost agrees with the case of a pure tilt, though dispersed a little.

Accordingly, the orientation relation is explained by the model with a kinetic point of view. As the orientation relation is characterized at the stage of growth, relatively large dispersion of the distribution of it is thought to be originated from two causes: Since anisotropy in kink-density does not change largely near highly kinked face, the growing grain boundary is capable of having many combinations of interfaces. The other is explained by considering the twist component of the grain boundary as mentioned here at the initial stage of the growth.

We need to check our growth model with experimental results when evaluating our discussions. The recrystallized grain changes its form during the growth due to anisotropy in growth rate, so that it is gradually bounded at the later stage by grain boundaries having low mobilities. The grain boundaries shown in Fig. 11 obtained from this experiment were actually those with low mobility. This confirms the validity of the growth model to a certain extent: Orientation of one slow migrating interface of the grains shown in Fig. 11 is near basal plane of the grown grain or the matrix, which does not have kink-site as listed in Table 3, so that the grain boundary follows to have the lowest mobility. This is a evidence certifying the model.

V. Concluding remarks

When discussing the formation mechanism of the preferred orientation of a polycrystal in glaciers, the result of this study is applicable with some success as follows: Recrystallization, which usually occurs at the grain boundary (Wakahama op. cit.; Suzuki, 1971), produces many fine recrystallized grains at the initial stage; therefore, this phenomena presents a good similarity to the present experiment. That is, the nucleation region in this experiment corresponds to the grain boundary in a polycrystal producing many fine recrystallized grains; the growth region of which corresponds to that of a grain. A recrystallized grain which appears in the grain boundary grows to one or both sides of the grain boundary with its c-axis characterized by the grain. The orientation relation obtained in this study shows a good agreement with the results of the misorientation angle between adjoining crystals in polycrystals. In this connection, Matsuda and Wakahama (1978) revealed that an outstanding peak can be seen between 40° and 50° in the frequency histogram of the angle between peaks of preferred c-axis orientations of the multi-maximum fabrics found and reported in many glaciers and ice sheets in the world. Huang et al. (1982) conducted a recrystallization experiment, in which they measured the misorientation angle between adjoining grains, showing that the frequency histogram of the misorientation gradually comes to have an outstanding peak at nearly 50° after repeating the recrystallization processes. These experimental results provide phenomenological verification of the validity of applying the present result to the case of the polycrystal.

VI. Acknowledgement

References

Akutsu, N. and Ookawa A. unpublished.

Aust, K. T. 1969 Grain Boundary Studies and their Technological Significance. *Can. Metall. Q.,* **8,** 173-178.

Bader, H. 1938 Mineralogische und Strukturelle Charakterisierung des Schnees und Seiner Metamorphose. *Schweizer Geol. Geotech. Ser. Hydrologie,* **3,** 1-61.

Beagehole, D. and Nason, D. 1980 Transition Layer on the Surface on Ice. *Surface Science,* **96,** 357-363.

Bolling, G. F. 1968 On the Average Large-Angle Grain Boundary. *Acta Met.,* **16,** 1147-1157.

Demianczuk, D. W. and Aust, K. T. 1975 Effect of Source and Orientation on the Mobility of Near-Coincidence Tilt Boundaries in High-Purity Aluminum. *Acta Met.,* **28,** 1149-1162.

Eisenberg, D. and Kauzmann, W. 1969 The Structure and Properties of Water, Oxford Univ. Press, London, 121.

Fletcher, N. H. 1970 The Chemical Physics of Ice, Cambridge Univ. Press, London, 106.

Gleiter, H. and Chalmers, B. 1972 Hihg-Angle Grain Boundaries (Chalmers, B., Christian, J. W., and Massalski, T. B. ed.) Pergamon Press, Oxford, 113-119.

Higashi, A. 1971 Kessyo Kougaku Handbook, Kyoritu Shuppan, Tokyo, 1081-1090.

Higashi, A., Matsuda M., Shoji H., and Ohtomo M. unpublished.

Huang M., Ohtomo, M., and Wakahama G. 1982 Takesso no kurikaesi saikesso jikken. [Repeated Recrystallization of Polycrystalline Ice] *Low Temperature Science Ser.* **A,** 41, 13-23.

Ibe, G. and Lücke, K. 1965 Growth Selection During Recrystallization of Single Crystals. *In* Recrystallization, Grain Growth, and Textures, ASM, Metals Park, Ohio, 434-447.

Kamb, B. 1959 Ice Petrofabric Observations from Blue Glacier, Washington, in Relation to Theory and Experiments. *J. Geophys. Res.,* **64,** 1891-1909.

Kamb, B. 1972 Experimental Recrystallization of Ice Under Stress. *Geophys. Mon. American Geophy. Union,* **16,** 211-241.

Ketcham, W. M. and Hobbs, P. V. 1969 An Experimental Determination of the Surface Energies of Ice. *Phil. Mag.,* **19,** 1161-1173.

Kizaki, K. 1962 Ice Fabric Studies on Hamna Ice Fall and Honnorbrygga Glacier, Antarctica. *Ant. Rec.,* **16,** 54-74.

Kizaki, K. 1969 Ice Fabric Study of the Mawson Region, East Antarctica. *J. Glaciol.,* **8,** 253-276.

Kizaki, K. 1969 Fabric Analysis of Surface Ice near Casey Range, East Antarctica. *J. Glaciol.,* **8,** 375-383.

Kronberg, M. L. and Wilson, F. H. 1949 Secondary Recrystallization in Copper. *Trans. Met. Soc. AIME,* **85,** 501-514.

Kuroda, T. and Lacmann, R. 1982 Growth Kinetics of Ice from the Vapour Phase and its Growth Forms. *J. Cryst. Growth,* **56,** 189-205.

Kuroiwa, D. and Hamilton, W. L. 1962 Studies of Ice Etching and Dislocation Etch Pits. *In* Snow and Ice, (W. D. Kingery ed.) MIT Press, Cambridge, Mass., 34-55.

Kvlividze, V. I., Kiselev, V. F., Kurzaev, A. B., and Ushakova, L. A. 1974 The mobile Water Phase on Ice Surface. *Surface Science,* **44,** 60-68.

Lücke, K., Rixen, R., and Rosenbaum, F. W. 1975 On the Theory of Grain Boundary Motion. *In* The Nature and Behaviour of Grain Boundaries, Plenum Press, New York, 245-283.

Matsuda, M. and Wakahama, G. 1978 Crystallographic Structure of Poltcrystalline Ice. *J. Glaciol.,* **21,** 607-620.

Perutz, M. F. and Seligman, G. 1939 A crystallographic Investigation of Glacier Structure and the Mechanism of Glacier Flow. *Proc. Roy. Soc. London, Ser. A,* **172,** 335-360.

Rigsby, G. P. 1951 Crystal Fabric Studies on Emmons Glacier, Mt. Rainier, Washington. *J. Geol.,* **59,** 590-598.

Rigsby, G. P. 1955 Study of Ice Fabrics, Thule Area, Greenland. *U. S. SIPRE, R. R.,* **26,** 1-6.

Rigsby, G. P. 1960 Crystal Orientation in Glacier and in Experimentally Deformed Ice. *J. Glaciol.,* **3,** 589-606.

Shumskii, P. A. 1958 The Mechanism of Ice Straining and its Recrystallization. *IASH,* **47,** 244-248.

Steinemann, S. 1958 Experimentalle Untersuchungen zur Plastizitat von Eis. Beitr. Geol.. *Hydologier* **10,** 46-50.

Suzuki, S. 1971 Kohri no assuku henkei de shojiru saikesso. [Recrystallization of Compressed Ice.] *Low Temp. Sci., Ser. A,* **29,** 11-28.

Turnbull, D. 1951 Theory of Grain Boundary Motion Rates. *Trans. Met. Soc. AIME,* **191,** 661-665.

Wakahama, G. 1964 Kohri no sosei henkei ni tsuite V. [On the Plastic Deformation of Ice V] *Low Temp. Sci., Ser. A,* **22,** 1-24.

Wakahama, G. 1965 Kohri no naibu hakai ni tsuite. [Internal Fracture of Ice] *Low Temp. Sci., Ser. A,* **23,** 39-50.

Watanabe, T. 1983 Observation of Plane-Matching Grain Boundaries by Electron Channeling Patterns. *Phil. Mag. A,* **47,** 141-146.

Wilson, C. J. L. and Russel-Head, D. S. 1982 Steady-State Preferred Orientation of Ice Deformed in Plane Strain at $-1°C$. *J. Glaciol.,* **28,** 145-160.

Yoshida, H., Liebmann, B., and Lücke, K. 1959 Orientation of Recrystallized Grains in Strained Aluminum Single Crystal. *Acta Met.,* **7,** 51-56.